Wind and Structures, Vol. 12, No. 5 (2009) 457-474
DOI: http://dx.doi.org/10.12989/was.2009.12.5.457

Fundamental restrictions for the closed-loop control of wind-loaded, slender bridges

Arno Kirch* and Udo Peil

Institute of Steel Structures, Technische Universität Carolo-Wilhelmina zu Braunschweig, Beethovenstraße 51, 38106 Braunschweig, Germany

(Received September 1, 2008, Accepted June 16, 2009)

Abstract. Techniques for stabilising slender bridges under wind loads are presented in this article. A mathematically consistent description of the acting aerodynamic forces is essential when investigating these ideas. Against this background, motion-induced aerodynamic forces are characterised using a linear time-invariant transfer element in terms of rational functions. With the help of these functions, the aeroelastic system can be described in the form of a linear, time-invariant state-space model. It is shown that the divergence wind speed constitutes an upper bound for the application of the selected mechanical actuators. Even active control with full state feedback cannot overcome this limitation. The results are derived and explained with methods of control theory.

Keywords: bridges; rational function approximation; state-space model; flutter; divergence; active control.

1. Introduction

New materials and innovative construction methods allow modern bridges to be built as very slender structures. This trend is accompanied by an increased susceptibility to oscillations. The design of extremely slender bridges, such as large-span road or filigree pedestrian bridges, is decisively influenced by their vibration behaviour. In this connection, special attention has to be given to wind-induced vibrations. In recent years, inspired also by aerospace engineering, a number of sophisticated techniques have been investigated to improve the vibration behaviour of bridges under the influence of wind with systematically imposed forces.

In theoretical, control-oriented investigations, external forces have often been applied without accounting for their origin (Meirovitch and Ghosh 1987, Miyata, *et al*. 1994, Pourzeynali and Datta 2005). Due to their intrinsic function, bridges only allow the use of specific actuating elements. It is preferred to consider girder-incorporated mechanical equipment that creates inertial or gyroscopic forces by moving masses. In recent years, theoretical investigations about attachments which are able to create additional aerodynamic forces have also been published (Wilde and Fujino 1998). This article is about the generation of moments with either gyroscopes or reaction wheels. For the controller design, the dynamic behaviour of these actuators is explicitly taken into account.

* Corresponding Author, E-mail: a.kirch@is.tu-braunschweig.de

The article is divided into three main sections. Section 2 addresses the dynamic characteristics of the aeroelastic plant. A brief mathematical description of the aerodynamic forces is first considered. Important terms of system theory are mentioned in this context. Subsequently, the state-space models of the actuator-free aeroelastic plant and the actuator-extended ones are derived. Their dynamic characteristics are analysed with parameter-dependent eigenvalue locations in the complex frequency plane. A two-dimensional system with structural properties similar to a bridge is provided to clarify all statements of this article in a comprehensible way. Section 3 deals with the controller design. After defining the design objectives, the possibility of closed-loop control is discussed. The structure of the loop is specified and the design algorithm is chosen. Accordingly calculated controller gains are analysed in detail. Finally, section 4 explains the dynamic characteristics of the closed loop.

2. State-space model and open-loop characteristics of the plant

2.1. Expressions for motion-induced aerodynamic forces

In order to investigate an aeroelastic bridge system with control theory methods, a realistic and mathematically consistent description of the forces caused by the wind flow around the girder is of particular importance. Usually, wind action is divided into several types of wind loads.

Together with its structural parameters, motion-induced wind forces influence the properties of an aeroelastic system. For a proper representation of the displacement-force relation, a transfer equation with a linear, time-invariant transfer element is used.

$$\mathbf{f}(p) = \mathbf{G}(p) \cdot \xi_s(p) \tag{1}$$

In Eq. (1) the aerodynamic force vector is denoted by $\mathbf{f}$ while the vector of the aerodynamically effective degrees of freedom is denoted by ξ_s. The transfer function $\mathbf{G}$ corresponds to the aerodynamic admittance of motion-induced wind forces. In this pure frequency-domain description, the values are to be regarded as unilateral Laplace transforms. The variable in the frequency domain p is the reduced complex frequency.

$$p = sb/U = (\sigma + i\omega)b/U = \beta + ik \tag{2}$$

The complex, non-reduced frequency in the Laplace domain is symbolised by s, b stands for the half width of the cross section according to the example system shown in Fig. 1 and U symbolises the constant horizontal mean wind speed. In aerospace engineering, a factor q_0, which includes the air density ρ, is usually separated from the transfer function of motion-induced forces. The following notation is the standard for most investigations on aeroservoelasticity problems of aircrafts and has been used since early publications on aerodynamics (Küssner and Schwarz 1940).

$$\mathbf{f}(p) = q_0 \cdot \mathbf{Q}(p) \cdot \xi_s(p), \; q_0 = \pi\rho b^2 U^2 \tag{3}$$

Thus, the matrix $\mathbf{Q}$ is only a function of the reduced complex frequency p. Its elements are called (aerodynamic) derivatives. In the following examples, the derivatives of the flat plate based on potential theory (Theodorsen 1934) are used for simplicity's sake. They are similar to derivatives of streamlined

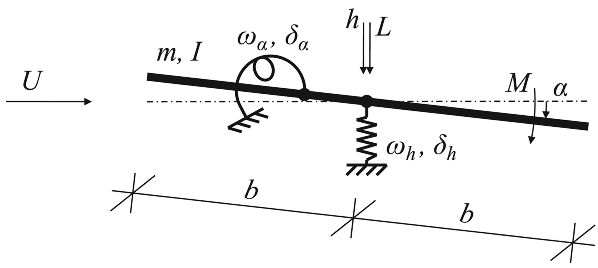

Fig. 1 Two-dimensional aeroelastic system with two aerodynamically effective degrees of freedom

bridge cross sections. For the two-dimensional aeroelastic system with two aerodynamically effective degrees of freedom h and α displayed in Fig. 1, the following detailed equation follows.

$$\begin{pmatrix} Lb \\ M \end{pmatrix}_{(p)} = \pi\rho b^2 U^2 \cdot \begin{pmatrix} Q_{11} & Q_{12} \\ Q_{21} & Q_{22} \end{pmatrix}_{(p)} \cdot \begin{pmatrix} h/b \\ \alpha \end{pmatrix}_{(p)} \tag{4}$$

According to Fig. 1, L is the vertical aerodynamic force and M is the resultant aerodynamic moment related to the middle of the deck. A dimensionless **Q**-matrix is obtained when using identical dimensions for both the different types of deformations and the different types of loads.

In civil engineering the Scanlan notation (Simiu and Scanlan 1996) is the preferred description of motion-induced forces. When introducing a harmonic approach into the Scanlan formula, the derivatives of Eq. (4) and the Scanlan derivatives can be directly compared for imaginary frequencies $p = 0+ik$.

$$\mathbf{Q}(ik) = \frac{k^2}{\pi}\begin{pmatrix} 2(H_4^*(k) + iH_1^*(k)) & 4(H_3^*(k) + iH_2^*(k)) \\ 4(A_4^*(k) + iA_1^*(k)) & 8(A_3^*(k) + iA_2^*(k)) \end{pmatrix} \tag{5}$$

The notation of the matrix elements in the right part of Eq. (5) or similar ones (Theodorsen and Garrick 1941) have several disadvantages compared with the elements of the **Q**-matrix. Since the reduced frequency k is separated, they cannot be seen as independent frequency-domain functions. This can lead to several mathematical problems and inconsistencies. A detailed discussion of these problems is very complex and not part of this article.

Similar to Eq. (1), gust-induced forces — or buffeting forces, as they are also called— which constitute another type of wind forces, can be connected with mean-value-free, fluctuating velocity components of gusts by aerodynamic gust admittances. Gust-induced forces will be only marginally mentioned here. Forces due to flow separation and vortex shedding are not considered here. Regarding the streamlined cross section, they are assumed to be negligible.

Usually, analytic functions of the complex frequency are taken to express the transfer function. With the aid of these functions, the derivatives of bridge cross sections, which are available for harmonic oscillations, are approximated. Rational functions are the most commonly used analytic transfer function approximations in aerospace engineering as well as in bridge engineering. In this article, rational functions according to the Minimum-State Method (Karpel 1981) are used.

$$\mathbf{Q}(p) = \mathbf{A}_0 + \mathbf{A}_1 p + \mathbf{A}_2 p^2 + \mathbf{D}(p\mathbf{I} - \mathbf{R})^{-1}\mathbf{E}p, \;\; \mathbf{R} = -\mathrm{diag}(\gamma_1, \gamma_2, \ldots, \gamma_{n_L}) \tag{6}$$

This approach is based on rational transfer functions with single, real poles ($-\gamma_i$), which are the same for all derivatives. Such approaches are particularly suitable for approximating the aerodynamic derivatives of girders with streamlined cross sections (Peil and Kirch 2008). The constant matrices $\mathbf{A}_1$, $\mathbf{A}_2$, $\mathbf{D}$ and $\mathbf{E}$ are determined with elaborate approximation procedures according to Tiffany Hoadley and Adams (1988). For the following examples, the derivative approximation is carried out with $n_L = 5$ poles. The result is given in Appendix II. Steady values of the derivatives are incorporated in the $\mathbf{A}_0$-matrix. The matching of the steady values is important for the evaluation of the divergence wind speed.

2.2. State-space model and characteristics of the actuator-free aeroelastic plant

After inserting Eq. (6) into Eq. (3) a part of the last summand of the resulting equation can be transformed into a linear differential equation with constant coefficients by introducing artificial so-called aerodynamic lag states ξ_a.

$$\xi_a = (p\mathbf{I} - \mathbf{R})^{-1}\mathbf{E}p\xi_s \quad \bullet\!\!-\!\!\!-\!\!\circ \quad \xi'_a - \mathbf{R}\xi_a = \mathbf{E}\,\xi'_s \tag{7}$$

The prime ( )' symbolises the generalised differentiation with respect to the non-dimensionalised time $\bar{t}$.

$$\bar{t} = \frac{U}{b}t \tag{8}$$

The time is denoted by t. Together with a linear structure description of the same kind,

$$\mathbf{M}_s\ddot{\xi}_s + \mathbf{C}_s\dot{\xi}_s + \mathbf{K}_s\xi_s = \mathbf{f} + \mathbf{u} + \mathbf{d}^d + \mathbf{d}^g \tag{9}$$

the aeroelastic system can be represented by a linear, time-invariant state-space model

$$\dot{\mathbf{x}} = \mathbf{A}\mathbf{x} + \mathbf{B}\mathbf{u} + \mathbf{E}^g\mathbf{d}^g + \mathbf{E}^d\mathbf{d}^d \tag{10a}$$

$$\mathbf{y} = \mathbf{C}\mathbf{x} \tag{10b}$$

where $\mathbf{x}$ is the state vector and ($\dot{}$) symbolises the generalised differentiation with respect to time t.

$$\mathbf{x} = (\dot{\xi}_s^{\mathrm{T}} \quad \xi_s^{\mathrm{T}} \quad \xi_a^{\mathrm{T}})^{\mathrm{T}} \tag{11}$$

Avoiding convolution integrals in the time domain is a major advantage of aerodynamic transfer functions in terms of rational functions. The matrices of the structural variables mass, damping and stiffness are denoted in these equations by $\mathbf{M}_s$, $\mathbf{C}_s$ and $\mathbf{K}_s$ respectively. $\mathbf{A}$ is the system matrix

$$\mathbf{A} = \begin{pmatrix} -\overline{\mathbf{M}}^{-1}\overline{\mathbf{C}} & -\overline{\mathbf{M}}^{-1}\overline{\mathbf{K}} & q_0\overline{\mathbf{M}}^{-1}\overline{\mathbf{D}} \\ \mathbf{I} & \mathbf{0} & \mathbf{0} \\ \mathbf{E} & \mathbf{0} & (U/b)\mathbf{R} \end{pmatrix} \tag{12}$$

where

$$\overline{\mathbf{M}} = \mathbf{M}_s - q_0(b/U)^2\mathbf{A}_2, \ \overline{\mathbf{C}} = \mathbf{C}_s - q_0(b/U)\mathbf{A}_1, \ \overline{\mathbf{K}} = \mathbf{K}_s - q_0\mathbf{A}_0. \tag{13}$$

In the state Eq. (10a) $\mathbf{d}^g$ and $\mathbf{d}^d$ represent the gust forces and other disturbance forces respectively. The control input $\mathbf{u}$ is important for the closed-loop control and is to be regarded in this section as external forces, which correspond to the structural degrees of freedom. The input matrices of the control input and the disturbances have the same entries.

$$\mathbf{B} = \mathbf{E}^g = \mathbf{E}^d = \left((\overline{\mathbf{M}}^{-1})^{\mathrm{T}} \ \mathbf{0}^{\mathrm{T}} \ \mathbf{0}^{\mathrm{T}} \right)^{\mathrm{T}} \tag{14}$$

The output equation (10b) cannot extract more than the structural states $\dot{\xi}_s$, ξ_s. In reality, the mathematically introduced lag states ξ_a cannot be measured. The mean horizontal wind speed U occurs in the system matrix $\mathbf{A}$ as a parameter. There are two reasons. The factor q_0 contains U (cp. Eq. (3)) and the generalised differentiation with respect to the absolute time symbolised by the dot $(\dot{\ })$ has to be used.

The dynamic characteristics of the aeroelastic system can be evaluated with an eigenvalue analysis of the system matrix $\mathbf{A}$. System stability is of major interest in this context. Due to the effect of motion-induced aerodynamic forces, aeroelastic instabilities can occur in the form of flutter and divergence. Unless otherwise explained, the two terms should specifically denote the cases of neutral stability. Since the system matrix contains the mean horizontal wind speed U, a parameter-dependent, linear eigenvalue problem must be solved.

The two-dimensional, generalised system in Fig. 1 is used as an example with the characteristic structural properties given in Table 1. The corresponding structural matrices are as follows:

$$\mathbf{M}_s = \begin{pmatrix} mb^2 & 0 \\ 0 & I \end{pmatrix}, \quad \mathbf{C}_s = \begin{pmatrix} c_h b^2 & 0 \\ 0 & c_\alpha \end{pmatrix}, \quad \mathbf{K}_s = \begin{pmatrix} k_h b^2 & 0 \\ 0 & k_\alpha \end{pmatrix} \tag{15}$$

Neutral stability appears at the zero crossings of the eigenvalue real-part curves (Fig. 2) as flutter at $U = 47.6$ m/s and as divergence at $U = 63.7$ m/s. This identification is possible when inspecting the eigenvalues and state eigenvectors. The indifferent flutter point occurs in two conjugate-complex eigenvectors with complex values. Its eigenfrequencies are purely imaginary and conjugate complex (Fig. 2). In the case of the flat plate, both structural degrees of freedom appear in the same order of magnitude, as can be predicted for the classical bending-torsional flutter. Indifferent divergence has only one eigenvector, the element values of which are real and vanish in the velocities $\dot{\xi}_s$ and in the lag states ξ_a. Its eigenfrequency is zero. In the case of uncontrolled bridges, the divergence wind speed is usually higher than the flutter wind speed and therefore normally not the focus of interest.

Table 1 Structural properties of the two-dimensional aeroelastic model

half deck width:	$b = 15.0$ m
mass:	$m = 25.0 \cdot 10^3$ kg/m
moment of inertia:	$I = 2.80 \cdot 10^6$ kgm^2/m
eigenfrequencies:	$\omega_h = 0.628$ 1/s
$k_h = \omega_h^2\, m$; $k_\alpha = \omega_\alpha^2\, I$	$\omega_\alpha = 1.13$ 1/s
logarithmic damping decrements:	$\delta_h = 0.0126$
$c_h = \delta_h\, m\, \omega_h / \pi$; $c_\alpha = \delta_\alpha\, I\, \omega_\alpha / \pi$	$\delta_\alpha = 0.0126$

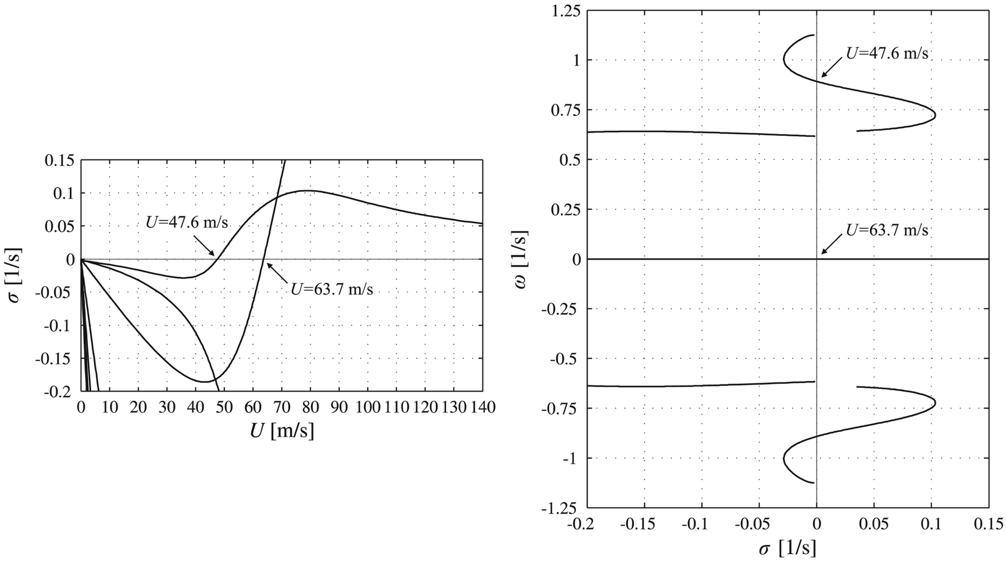

Fig. 2 Eigenvalues of the actuator-free aeroelastic system

This statement does not hold up when actuators are applied.

The following sections explain how and within what limits the system characteristics can be changed.

2.3. State-Space Model and Open-Loop Characteristics of the Extended Aeroelastic Plant

As has been mentioned in the introduction, actuators are considered which impose torques on the bridge deck by rotating masses around their centre of gravity (Fig. 3). For instance in contrast to masses that are moved in a vertical direction, no mechanical work due to gravity must be done, that is impossible to be regained without dissipation. In addition, rotational solutions seem to be easier to implement in practice. Control moment gyroscopes (CMG) and reaction wheels have been

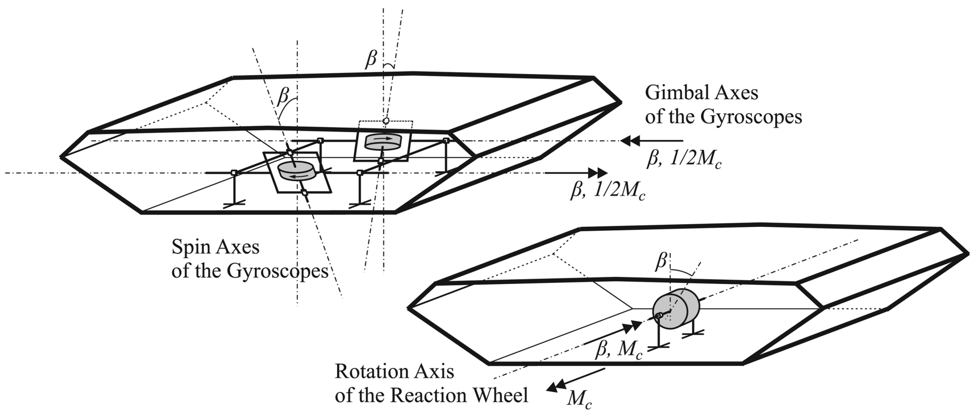

Fig. 3 Twin control moment gyroscope and reaction wheel as actuating devices in a bridge girder

employed for attitude control of satellites for a long time (Jacot and Liska 1966). Gyroscopes are also used to counteract the rolling of ships (Ferry 1932). The gyroscopic stabilisation of airfoils is described in Buchek (1974). In bridge engineering, the application of gyroscopes has repeatedly been analysed (Murata and Ito 1971, Fujisawa 1995, Okada, *et al*. 2001, Okada, *et al*. 2003). The use of reaction wheels for enhancing the flutter wind speed of bridges is proposed in Miyata, *et al*. (1994) and was experimentally investigated by Körlin and Starossek (2007) in a wind tunnel.

In comparison to reaction wheels, gyroscopes possess the disadvantage of needing a spin to create an angular momentum. However, they feature the well-known amplification effect between the moment around the gimbal axis and the generated torque in the perpendicular direction. The latter is used for the control input of the aeroelastic system. A twin CMG (Fig. 3), which is a well-known and commercially available special kind of a CMG (cp. references given before), features the possibility of creating resulting gyroscopic moments around a fixed axis. For this purpose, both gyroscopes spinning in opposite directions with the same angular momentum must be simultaneously tilted around equal but opposite gimbal angles. The structural properties of the actuating elements that are used in this article are shown in Table 2. The physical values of the discrete actuators have already been divided by their distance perpendicular to the considered plane of the aeroelastic system. In order to simplify the analysis, the inertia of the gimbal is neglected.

When applying principles of mechanics, the motion equations of the actuator-extended plant (Fig. 4) can be derived. In the case of the twin CMG, as it is customary in engineering applications, the gyroscope equations are simplified and linearised for small tilt angles. As a result, ξ_s is enlarged with an aerodynamically non-effective structural degree of freedom β.

Table 2 Structural properties of the actuating devices

twin CMG (gy)	
double mass of one gyro:	$m_{gy} = 1.25 \cdot 10^3$ kg/m
double moment of inertia of one gyro around its spin axis:	$I_{gy,sp} = 1.13 \cdot 10^4$ kgm²/m
double moment of inertia of one gyro around the gimbal axis:	$I_{gy,gi} = 5.63 \cdot 10^3$ kgm²/m
angular speed of one gyro around its spin axis:	$\Omega = 28.2$ 1/s
reaction wheel (rw)	
mass:	$m_{rw} = 1.25 \cdot 10^3$ kg/m
moment of inertia:	$I_{rw} = 1.13 \cdot 10^4$ kgm²/m

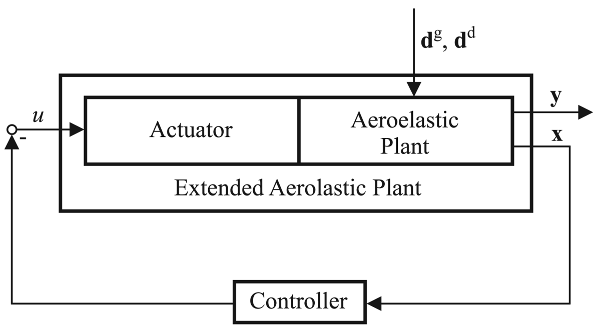

Fig. 4 Block diagram of the system structure

$$\xi_s = (\,h/b \quad \alpha \quad \beta\,)^{\mathrm{T}} \tag{16}$$

The angle β symbolises the rotation of the reaction wheel relative to the bridge deck or the tilt angle of one CMG gimbal (Fig. 3). The matrices and vectors of the preceding paragraphs must be suitably expanded with zeros. Moreover, the following matrices must be added. The indices (gy) and (rw) represent the CMG and the reaction wheel respectively.

$$\mathbf{M}_{s,\,gy} = \begin{pmatrix} m_{\mathrm{gy}}b^2 & 0 & 0 \\ 0 & I_{\mathrm{gy,\,gi}} & 0 \\ 0 & 0 & I_{\mathrm{gy,\,gi}} \end{pmatrix} \qquad \mathbf{M}_{s,\,rw} = \begin{pmatrix} m_{\mathrm{rw}}b^2 & 0 & 0 \\ 0 & I_{\mathrm{rw}} & I_{\mathrm{rw}} \\ 0 & I_{\mathrm{rw}} & I_{\mathrm{rw}} \end{pmatrix} \tag{17a}$$

$$\mathbf{C}_{s,\,gy} = \begin{pmatrix} 0 & 0 & 0 \\ 0 & 0 & \Omega I_{\mathrm{gy,\,sp}} \\ 0 & -\Omega I_{\mathrm{gy,\,sp}} & 0 \end{pmatrix} \tag{17b}$$

Table 2 shows the definition of the physical values that occur in the matrices of Eq. (17a) and Eq. (17b). In the mass matrix of the reaction wheel, there are non-zero off-diagonal elements due to the relative definition of the angle β. Since the dynamic behaviour of the actuator is explicitly taken into account, the abstract control input **u** in Eq. (9) and Eq. (10) must be replaced by the input of the actuating elements.

$$\mathbf{u} = (\,0 \quad 0 \quad M_c\,)^{\mathrm{T}} \tag{18}$$

Hence, the control input can be set as a scalar value. The input matrix must be modified accordingly.

$$\tilde{\mathbf{B}} = \mathbf{B}(\,0 \quad 0 \quad 1\,)^{\mathrm{T}}, \qquad \tilde{u} = M_c \tag{19}$$

In the case of the reaction wheel, the control input M_c signifies the driving torque that acts on the wheel and is based on the bridge girder. When extending the aeroelastic plant with a twin CMG, the input is generated by a torque between the two tilting gimbal axes (Fig. 3). The dynamic behaviour of sensors and other actuators is neglected in this article because they are assumed to be fast compared to the components of the extended plant investigated here.

The actuating elements modify the eigenvalue curves of the actuator-free aeroelastic system (Figs. 5 and 6). As their additional degree of freedom is freely movable in the open loop at least in a quasi-static sense, they introduce new, neutral-stable eigenvalues into the origin of the frequency plane. By just adding its mass, the reaction wheel has only a little effect on the curves. Its absolute rotational degree of freedom is not excited in the open loop because it is not coupled with the main system. As expected, β appears in the flutter eigenvector with the same absolute value as the torsional displacement α of the girder and a relative phase shift of π, which is due to its relative definition. Contrary to this, the twin CMG noticeably alters the characteristics of the aeroelastic system by gyroscopic coupling. The flutter wind speed is thus theoretically increased to $U =$ 137.6 m/s. For this high wind speed, the assumption of a constant air density made by Theodorsen (1934) for the aerodynamic forces is not valid anymore. Effects of compressibility are, however, not

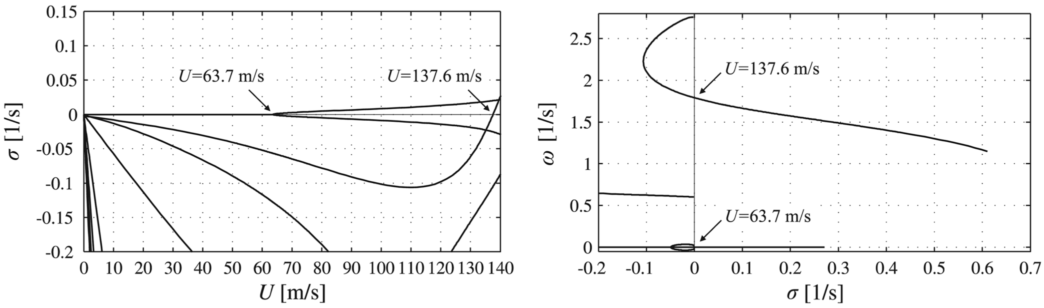

Fig. 5 Eigenvalues of the aeroelastic system extended with a twin CMG

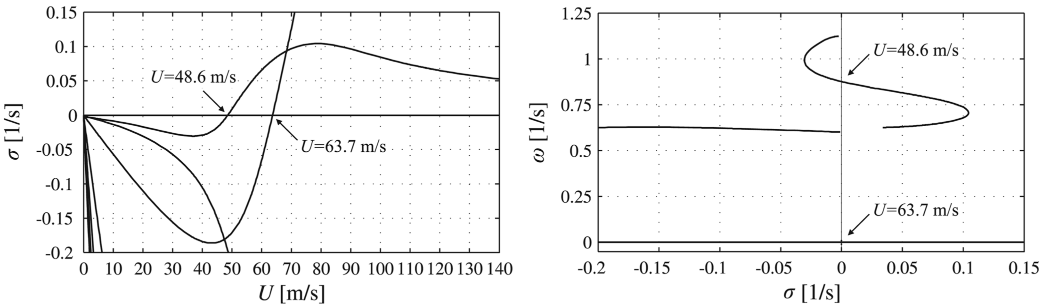

Fig. 6 Eigenvalues of the aeroelastic system extended with a reaction wheel

included in these investigations. The flutter eigenvector is dominated by the gyroscopic degree of freedom. However, both actuators do not influence the divergence wind speed and its eigenvector at all. In this section, the following explanation should be sufficient: Especially gyroscopes only change the dynamic parameters of the aeroelastic system but not its static ones, which are responsible for this type of failure.

Because of their rigid body motion, both actuating systems are useless when they are applied without further couplings. In this way, even CMGs cannot ensure a minimum of stability. Disturbances acting on the extended aeroelastic plant produce undamped rotations of the gyroscopes around their gimbal axes with large amplitudes, which in turn negatively affect the aeroelastic system. Furthermore, the large rotations do not correspond with the assumptions that have been made for the linearisation of the gyroscope equations.

To systematically influence the aeroelastic system, the inputs of the extended plant must depend on its outputs or states. Hence, the control loop must be closed. In so doing, the rigid body motion of the actuating devices is eliminated as well.

3. Controller design

3.1. Design objectives

The objective of a closed-loop control is to force a plant to behave in a desired manner. For bridges, controller design aims at disturbance rejection. Acting disturbances should excite the system states or the measured plant output as little as possible. In addition to technical feasibility and economic efficiency, the design should fulfil a set of requirements. For instance, the transient and the steady-state response of the closed loop under the influence of disturbances should occur within predefined limits. In this article, the design is only carried out with respect to zero-mean, time-varying disturbances. Problems arising for example as a result of disturbances in the form of step functions necessitate advanced controller design techniques. Furthermore, the controller must be sufficiently robust against uncertainties of the plant model. Multivariable controllers should feature integrity properties. That means, even if some sensor or control signals fail, the stability of the closed loop must be ensured. Due to the occurring instabilities, the guarantee of a certain level of stability is particularly important for aeroelastic plants. This article addresses stabilisation limits of aeroelastic systems when the above mentioned actuating elements are used. Hence, here it is sufficient to design the controller only with respect to a specific stability level. The term vibration control — in other words manipulating complex-conjugate eigenvalues of the system matrix — describes only a sub-objective of the mentioned main design objective stabilisation. When stabilising a plant, all eigenvalues that are located in undesired positions must be taken into account.

3.2. Controllability and observability of the extended plant

Controllability and observability are basic characteristics of a dynamic system which crucially influence the feasibility of closed-loop control. Only the part of a plant that is both controllable and observable can be controlled in a closed loop. The Hautus criteria (Hautus 1969), which are commonly known in control theory, are well-suited tools to examine these properties. They not only allow statements to be made about the controllability or observability of a system, but also whether a particular eigenvalue has these properties. When using the Minimum-State Method for approximating the derivatives of motion-induced aerodynamic forces, all eigenvalues of the extended plant investigated here are generally controllable by the chosen input M_c. Exceptions are described in section 3.4. As is known, the actuator torque can also influence the vertical bridge motion because of the aerodynamic coupling of the aeroelastic system. If the output signals are selected appropriately, the extended system is completely observable as well. For this purpose, apart from exceptions described in section 3.4, the output of the actuator angle β is sufficient.

When using other methods for rational approximation of the transfer function of motion-induced aerodynamic forces according to Roger (1977) and Abel (1979) non-controllable eigenvalues occur for the case of the theoretically described flat plate. Their occurrence can be explained with parallel subsystems within the state-space model due to the other way of approximation. The non-controllable eigenvalues are, however, located in the stable, left part of the complex frequency plane and do not need to be stabilised. After transforming the state-space model into its canonical form, the non-controllable states can be separated. Then the controller can be designed for the controllable part of the plant. All results presented in this article can be derived by this approximation alternative as well. Any associated stumbling blocks are not addressed here.

3.3. Closed-loop structure and controller design method

Several controller types are available. Passive controllers can be considered in view of control theory as an output feedback that, moreover, cannot introduce energy into the plant. Spring-damper systems, for instance, connect specific outputs of the extended aeroelastic plant like β and $\dot{\beta}$ to the control input M_c. Tuned mass dampers use this concept (Lin, *et al.* 1999, Pourzeynali and Datta 2002). Due to their dissipative nature and the insufficiencies associated with output feedback, the ability of passive controllers for system stabilisation is foreseeably limited. Semi-active controllers are also passive instruments whose parameters, like damping property, can be modified. Hence, they offer the possibility to change the controller parameters corresponding to the varying aeroelastic plant parameter, i.e. the mean horizontal wind speed U. Nonetheless, they still exhibit the principal shortcomings of passive controllers.

In contrast, active controller systems allow for energy input into the plant and, when combined with state feedback, they are the most favourable controller type concerning stabilisation. They are therefore dealt with in the following sections. Safety aspects of active stabilisation in permanent operation are not regarded here. At least for construction stages of bridges with undesirable aeroelastic characteristics, active controllers are considered to be a useful option. As has already been shown in the equations of motion of the extended aeroelastic plant — apart from the gyroscopic coupling in the case of the CMG — there is no structural coupling between the rotations of the actuator and the bridge when using pure active control. For practical applications, it is reasonable to replace parts of the controller gains by structural components such as viscous dampers or springs. These hybridly controlled systems are not regarded here.

When closing the control loop with a linear, proportional controller, stability can again be examined by regarding its eigenvalues. In order to ensure that the design objectives are achieved, the controller gain is calculated for closely spaced discrete nodes of the parameter value U of the plant and cubically interpolated afterwards. This gain scheduling can be considered as an adaptive control with one drawback. As gain scheduling has no feedback of the actual system behaviour, an incorrect schedule cannot be compensated (Åstrom and Wittenmark 1995).

The feedback of the state vector

$$\mathbf{u} = -\mathbf{K}\mathbf{x} \tag{20}$$

combined with the method of pole assignment allows all controllable eigenvalues to be placed individually, even if only one system input is available.

$$\tilde{u} = -\mathbf{k}^{\mathrm{T}}\mathbf{x} \tag{21}$$

As has been explained above, it is impossible to measure, in particular, the artificial aerodynamic states ξ_a. However, state estimators like Kalman filter or Luenberger observer can reconstruct the state from the output provided that the system is realistically modelled and observable by its output. As a result of the separation theorem, the mentioned estimators do not modify the closed-loop eigenvalues that are based on state feedback. The design of the state estimator is not dealt with in this study.

Several methods of pole assignment are described in the available literature, but in the case of a single input, they should all produce the same solution. For the examples in this article, the algorithm of Kautsky and Nichols (1985) is used because it offers reliable numeric results. Since the controller is only designed for a certain level of stability, the following procedure is sufficient: All eigenvalues that are placed to the right of a selected bound $\sigma_{\max}$ are shifted to this bound by keeping its imaginary values constant. The value is set at $\sigma_{\max} = -0.113$ 1/s.

3.4. Properties of the controller vector

Fig. 7 shows the graph of one element of the calculated controller matrices that connects the angle β of the actuator with the input M_c of the extended plant. The behaviour of this element is typical of the controller. Its values are displayed starting from a horizontal mean wind speed of $U = 15.0$ m/s. Below this speed, the aerodynamic coupling of the vertical and torsional motion of the bridge deck decreases considerably. The resulting degradation of controllability is compensated by higher controller gains.

The graphs can be separated into two parts on both sides of the pole-like singularity. Visible kinks in both parts occur at wind speeds where eigenvalue curves cross the selected stability level. At flutter wind speeds of the extended plants, no distinctive behaviour of the controller graph appears. Therefore, the crossing of the imaginary axis by conjugate-complex eigenvalues constitutes no significant point for the dimensioning of the controller. In contrast, the divergence wind speed marks a singularity for the controller values. As described above, this instability has not been changed when extending the aeroelastic plant. The controller values show the mentioned pole behaviour around it. The higher the chosen stability level, the wider the pole area.

The phenomenon can be explained by using Hautus' controllability criterion. Exactly when the neutral stability of aeroelastic divergence occurs, i. e. an eigenvalue is located at the origin of the complex frequency plane, this eigenvalue is not controllable. Therefore, it cannot be stabilised in a closed loop. When approaching the divergence wind speed, the controllability of the plant decreases. The pole assignment algorithm tries to compensate this by increasing the controller gain. This value thus tends to go to infinity when the controllability singularity is reached. Though it is not of primary interest to state feedback, it should be noted that observability is not given in the case of aeroelastic divergence either if only the relative motion (β and $\dot{\beta}$) of the actuators is measured.

For the neutral stability of divergence, in addition to damping, the stiffness vanishes. The mechanical actuating elements, which are addressed here, are only linked to the system and do not modify this zero stiffness. The motion of the divergence mode is equivalent to a rigid body motion whose impulse can be internally exchanged by internal forces but not reduced. Without stiffness, it is also not possible to define an equilibrium position that is independent of the chosen coordinate system. Without a physically based equilibrium position, it is in turn not possible to define an asymptotic stable behaviour for the extended plant. This also explains why the extension of the aeroelastic plant with the actuators has not altered the divergence wind speed.

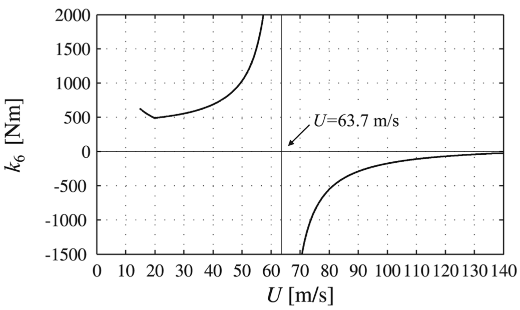

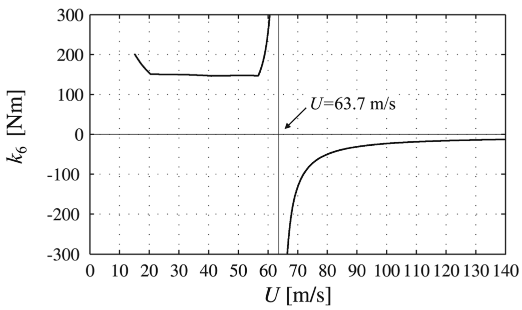

Fig. 7 Controller gain for the extended aeroelastic plant; extended with twin CMG on the left, extended with reaction wheel on the right

In contrast, when imposing an external actuating moment on the bridge, this moment can also change the system impulse for the divergence wind speed and a zero position can be defined. Hence, controllability is ensured for all wind speeds. There is no singularity in the controller behaviour. Therefore the problem does not appear in the papers that are mentioned in the introduction. The authors of this article have recently explored if analogous problems occur for aeroelastic systems that are stabilised by additional aerodynamic forces (Kirch, *et al*. 2009a/b).

In the work by Körlin and Starossek (2004) and Körlin and Starossek (2007), the state of the reaction wheel is not included in the feedback loop. To avoid uncontrolled and non-vanishing angular speeds, the angle itself and its speed must, however, be incorporated in the state vector. For this purpose, a mathematically motivated actuator model in terms of combined PT_3 elements can be applied if a displacement input is chosen (Kirch, *et al*. 2009a/b). As explained before, an aeroelastic system looses its static stiffness when it is affected by a wind flow with divergence speed. The influence of a disturbance with a constant value will provoke a constant angular acceleration of the reaction wheel if the approach of the mentioned authors is used. Hence, instability is only shifted from the aeroelastic system to the reaction wheel. The aeroelastic system is thus not stabilisable with this actuator type for the divergence wind speed. The result corresponds to the conclusions of this article and has not been described in the cited papers.

The controller values below and above the divergence wind speed differ in sign. Similar phenomena can be found if conservative systems are stabilised by gyroscopic forces (Seyranian, *et al*. 1995).

4. Characteristics of the closed-loop system

By inserting the feedback Eq. (21) into the state Eq. (10a) of the extended plant, the behaviour of the closed-loop-controlled system can be simulated. The dynamic characteristics of the controlled system can again be found with an eigenvalue analysis of its system matrix.

$$\mathbf{A}_{\mathrm{cl}} = \mathbf{A} - \tilde{\mathbf{B}}\mathbf{k}^{\mathrm{T}} \tag{22}$$

Figs. 8 and 9 show the eigenvalue curves. As expected, the controllers move the low-damped or instable parts of the curves to the selected level of the frequency real part except for wind speeds around the aeroelastic divergence. Due to interpolation deficiencies of the controller gain, the instability of the closed loop occurs slightly below the divergence wind speed of the plant and

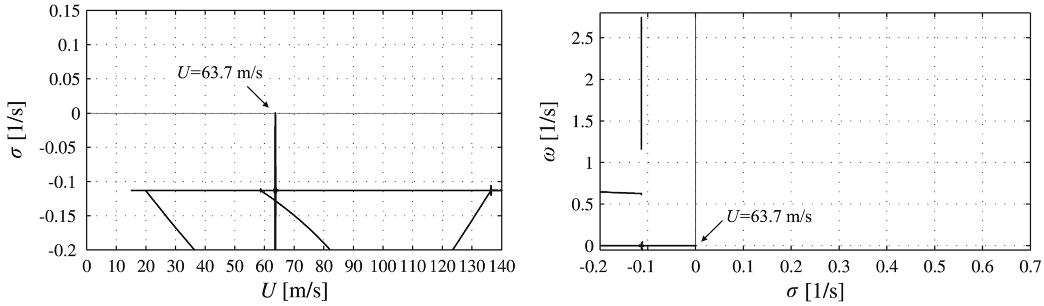

Fig. 8 Closed-loop eigenvalues of the aeroelastic system extended with a twin CMG

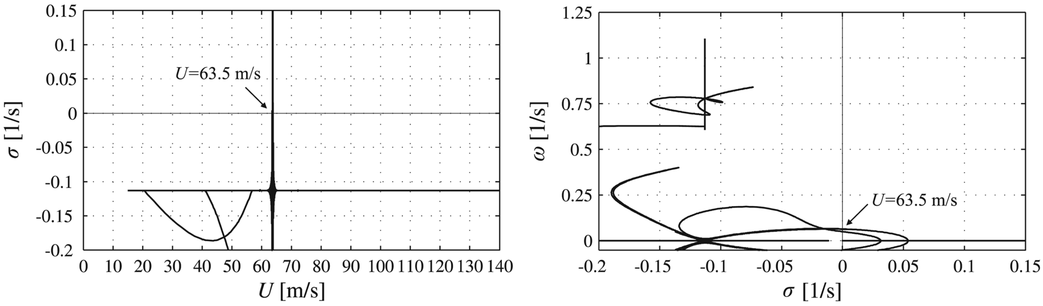

Fig. 9 Closed-loop eigenvalues of the aeroelastic system extended with a reaction wheel

disappears slightly above it. When applying the reaction wheel, the loop is so sensitive that the interpolation causes a noticeable drop below the required damping level. In Fig. 9 this lack of robustness causes the noose-like eruptions of the eigenvalue curves. A powerful sorting algorithm for the calculated eigenvalues allows these curves to be determined. Of course, active controllers in contrast to passive ones are able to stabilise the plant above the divergence wind speed as well. If twin CMGs are used, neutral stability appears in the form of divergence, which is dominated by the actuator displacement. When employing reaction wheels, indifferent stability has a flutter mode with a distinct wheel rotation. Because of its low frequency, this dynamic behaviour is similar to a divergence. Interpolation effects are again the reason why there is no pure divergence.

The high feedback gains around the divergence wind speed can technically be achieved to a certain extent only. When lowering the required stability level, the width of the pole areas can be narrowed. It could be argued that a very narrow, instable speed interval is not relevant in reality. But as a result of modelling errors, the divergence wind speed is associated with uncertainties. In combination with the step-like change of sign of the controller values, the plant remains unstable in a still non-negligible interval. Even advanced adaptive control strategies with feedback of the plant behaviour are likely to fail due to these problems.

Based on all these explanations, the divergence wind speed of the aeroelastic system must be regarded for the two investigated mechanical actuators as an upper bound even when using active control.

All conclusions that are drawn in this article are based on a linear description of the aeroelastic system. The question whether the results can be changed when including structural and aerodynamical nonlinearities is not answered here.

5. Conclusions

In this article, stabilisation of a linear aeroelastic system by both inertial and gyroscopic forces has been theoretically investigated. For this purpose, a reaction wheel and a twin control moment gyroscope have been applied. It has been shown that the divergence wind speed, unlike the flutter wind speed, constitutes a fundamental limit for the application of these instruments. Even the more theoretical but in terms of stabilisation most favourable use of active control by full-state feedback cannot overcome this shortcoming. Two substantial facts motivate this statement: On the one hand, the indifferent divergence eigenvalue cannot be controlled with the mentioned actuators. On the other hand, the controller characteristics below and above the indifferent divergence wind speed differ significantly from each other. Within a non-negligible interval around the divergence wind speed a sufficient robustness of the closed-loop stability does not seem to be realisable.

Similar fundamental limits of other types of actuating devices still remain to be examined. Further investigations should also clarify if and how the consideration of the nonlinear plant behaviour can weaken the conclusions of this article.

Acknowledgements

We gratefully acknowledge the support given to this work by the International Graduate College IGC 802 of the German Research Foundation (DFG).

References

Abel, I. (1979), "An analytical technique for predicting the characteristics of a flexible wing equipped with an active flutter-suppression system and comparison with wind-tunnel data", NASA-TP-1367, Technical Paper, NASA.

Åstrom, K.H. and Wittenmark, B. (1995), *Adaptive Control*, 2nd Edition, Addison-Wesley, Reading, Massachusetts.

Buchek, P.M. (1974), "Modern control techniques in active flutter suppression using a control moment gyro", NASA-CR-138494, Contractor Report, NASA.

Ferry, E.S. (1932), *Applied Gyrodynamics*, Wiley, New York.

Fujisawa, N. (1995), "Control of coupled flutter of a bridge deck by mechanical damper", *50th Annual Conf. of the Japan Society of Civil Engineers*, Tokyo, Japan, 1508-1509, (in Japanese).

Hautus, M.L.J. (1969), "Controllability and observability conditions of linear autonomous systems", *Indagationes Mathematicae*, **31**, 443-448.

Jacot, A.D. and Liska, D.J. (1966), "Control moment gyros in attitude control", *J. Spacecraft Rockets*, **3**(9), 1313-1320.

Karpel, M. (1981), "Design for active and passive flutter suppression and gust alleviation", NASA-CR-3482, Contractor Report, NASA.

Kautsky, J. and Nichols, N.K. (1985), "Robust pole assignment in linear state feedback", *Int. J. Control*, **41**, 1129-1155.

Kirch, A., Peil, U. and Borri, C. (2009a), "Limits for the control of wind-loaded slender bridges with movable flaps; Part I: Aerodynamic modelling, state-space model and open-loop characteristics of the aeroelastic system", *EACWE 5 - Proc. of the 5th European and African Conf. on Wind Engineering EACWE 5*, Florence, Italy.

Kirch, A., Peil, U. and Borri, C. (2009b), "Limits for the control of wind-loaded slender bridges with movable flaps; Part II: Controller design, closed-loop characteristics of the aeroelastic system and gust alleviation", *EACWE 5 - Proc. of the 5th European and African Conf. on Wind Engineering EACWE 5*, Florence, Italy.

Körlin, R. and Starossek, U. (2004), "Active mass dampers for flutter control of bridges", *Proc. of the 8th Int. Conf. on Flow-Induced Vibration*, Paris, France.

Körlin, R. and Starossek, U. (2007), "Wind tunnel test of an active mass damper for bridge decks", *J. Wind Eng. Ind. Aerod.*, **95**(4), 267-277.

Küssner, H.G. and Schwarz, L. (1940), "Der schwingende Flügel mit aerodynamisch ausgeglichenem Ruder", *Luftfahrtforschung*, **17**, 337-354 (in German).

Lin, Y., Cheng, C. and Lee, C. (1999), "Multiple tuned mass dampers for controlling coupled buffeting and flutter of long-span bridges", *Wind Struct.*, **2**, 267-284.

Meirovitch, L. and Ghosh, D. (1987), "Control of flutter in bridges", *J. Eng. Mech.*, **113**(5), 720-736.

Miyata, T., Yamada, H., Dung, N.N. and Kazama, K. (1994), "On active control and structural response control of the coupled flutter problem for long span bridges", *First World Conf. on Structural Control*, Los Angeles, WA4-40 – WA4-49.

Murata, M. and Ito, M. (1971), "Suppression of wind-induced vibration of a suspension bridge by means of a gyroscope", *Third Int. Conf. on Wind Effects on Buildings and Structures*, Tokyo, 1057-1066.

Okada, T., Honke, K., Sugii, K. and Shimada, S. (2003), "Aerodynamic stability improvements in super-long-span suspension bridge through the use of gyroscopic dampers", Kobe Steel Engineering Reports, **53**(1), 59-63, (in Japanese).

Okada, T., Honke, K., Sugii, K., Shimada, S. and Kobayashi, H. (2001), "Suppression of coupled flutter of a bridge deck by gyroscopic damper", *IABSE Conf. on Cable-Supported Bridges*, Seoul, South Korea.

Peil, U. and Kirch, A. (2008), "Approximation of unsteady aerodynamic derivatives by rational functions", *EURODYN 2008 - 7th European Conf. on Structural Dynamics*, Southampton, UK, Paper E181.

Pourzeynali, S. and Datta, T.K. (2002), "Control of flutter of suspension bridge deck using TMD", *Wind Struct.*, **5**, 407-422.

Pourzeynali, S. and Datta, T.K. (2005), "Control of suspension bridge flutter instability using pole-placement technique", *J. Sound Vib.*, **282**, 89-109.

Roger, K. (1977), "Airplane math modelling methods for active control design", *Structural Aspects of Active Controls - AGARD Conf. Proceedings*, **228**, 4-1–4-11.

Seyranian, A., Stoustrup, J. and Kliem, W. (1995), "On gyroscopic stabilization", *Zeitschrift für angewandte Mathematik und Physik*, **46**, 255-267.

Simiu, E. and Scanlan, R.H. (1996), *Wind Effects on Structures: Fundamentals and Applications to Design*, 3rd Edition, Wiley, New York.

Theodorsen, T. (1934), "General theory of aerodynamic instability and the mechanism of flutter", NACA TR-496, Technical Report, NACA.

Theodorsen, T. and Garrick, I.E. (1941), "Nonstationary flow about a wing-aileron-tab combination including aerodynamic balance", NACA TR-736, Technical Report, NACA.

Tiffany Hoadley, S. and Adams Jr., W.M. (1988), "Nonlinear programming extensions to rational function approximation methods for unsteady aerodynamic forces", NASA-TP-2776, Technical Paper, NASA.

Wilde, K. and Fujino, Y. (1998), "Aerodynamic control of bridge deck flutter by active surfaces", *J. Eng. Mech.*, **124**(7), 718-727.

CC

Appendix I. Notation

The following symbols are used in this paper. Tables 1 and 2 define additional variables.

$\mathbf{f}$	vector of motion-induced aerodynamic forces
$\mathbf{G}$	matrix of the aerodynamic transfer function or aerodynamic admittance function of motion-induced aerodynamic forces
ξ_s	vector of structural degrees of freedom containing aerodynamically effective ones and if needed others like the actuator degree of freedom
p	reduced complex frequency
i	imaginary unit; $i^2 = -1$
β, k	real and imaginary part of the reduced complex frequency
s	complex frequency
σ, ω	real and imaginary part of the complex frequency
U	horizontal mean wind speed
b	half width of the aerodynamically effective cross section
q_0	factor in the aerodynamic transfer equation
ρ	air density (≈ 1.25 kg/m^3)
$\mathbf{Q}$	matrix of aerodynamic derivatives
L, M	motion-induced aerodynamic vertical force and moment acting on the example system (Fig. 1)
h, α	structural degrees of freedom of the example system (Fig. 1)
H_i^*, A_i^*	aerodynamic derivatives according to Simiu and Scanlan (1996)
$\mathbf{A}_i$, $\mathbf{D}$, $\mathbf{E}$, $\mathbf{R}$	matrices of the rational function approximation
$\mathbf{I}$	identity matrix
γ_i	elements on the main diagonal of $\mathbf{R}$
n_L	order of the square matrix $\mathbf{R}$ and total number of poles for the rational function approximation
ξ_a	vector of aerodynamic states
t, $\bar{t}$	time and non-dimensionalised time
$\dot{(\ )}$, $(\ )'$	generalised differentiation with respect to the time t and the non-dimensionalised time $\bar{t}$
$\mathbf{M}_s$, $\mathbf{C}_s$, $\mathbf{K}_s$	structural matrices of mass, viscous damping and stiffness
$\overline{\mathbf{M}}$, $\overline{\mathbf{C}}$, $\overline{\mathbf{K}}$	matrices of mass, viscous damping and stiffness including aerodynamic effects
$\mathbf{A}$, $\mathbf{C}$	system matrix and output matrix of the state-space model
$\mathbf{x}$, $\mathbf{y}$	state vector and output vector of the state-space model
$(\ )^{\mathrm{T}}$	transposition
$\mathbf{u}$, $\mathbf{d}^g$, $\mathbf{d}^d$	vector of the control input, the gust forces and other disturbance forces
$\mathbf{B}$, $\mathbf{E}^g$, $\mathbf{E}^d$	input matrices of the state-space model relating to control input, gust forces and other disturbance forces
$\tilde{\mathbf{B}}$, $\tilde{u}$	modified input matrix and control input
β	rotational angle of the reaction wheel relative to the bridge deck; tilt angle of one CMG gimbal
M_c	driving torque on the reaction wheel, based on the bridge deck or generated torque between the two tilting gimbal axes of a twin CMG

$\mathbf{K}$, $\mathbf{k}$	feedback gains
σ_{max}	intended maximal value of the eigenvalue real parts of the controlled system
$\mathbf{A}_{cl}$	system matrix of the controlled system

Appendix II. Rational function approximation for the theoretical derivatives of the flat plate

$$\mathbf{A}_0 = \begin{pmatrix} 0 & -2 \\ 0 & 1 \end{pmatrix}; \quad \mathbf{A}_1 = \begin{pmatrix} -1.00 & -1.50 \\ 0.50 & -0.25 \end{pmatrix}; \quad \mathbf{A}_2 = \begin{pmatrix} -1.00 & -0.00 \\ -0.00 & -0.125 \end{pmatrix};$$

$$\mathbf{D} = \begin{pmatrix} 4.00 & 4.00 & 4.00 & 4.00 & 4.00 \\ -2.00 & -2.00 & -2.00 & -2.00 & -2.00 \end{pmatrix}; \quad \mathbf{E} = \begin{pmatrix} -0.01315 & 0.13275 \\ -0.06519 & 0.15000 \\ 0.08686 & -0.20937 \\ -0.10831 & 0.23758 \\ 0.03755 & -0.09280 \end{pmatrix};$$

$$\mathbf{R} = -\mathrm{diag}(0.08600 \quad 0.48621 \quad 0.89432 \quad 1.20274 \quad 1.49171)$$